Proceedings of the ASME 2009 Dynamic Systems and Control Conference
DSCC2009
October 12-14, 2009, Hollywood, California, USA

DSCC2009-2641

A Base -Excitation Approach to Polynomial Chaos-Based Estimation of Sprung Mass for Off-Road Vehicles

Benjamin L. Pence[1], Hosam K. Fathy[2], and Jeffrey L. Stein[3]

(1) Graduate Student, (2) Assistant Research Scientist, (3) Professor,
Mechanical Engineering Department, The University of Michigan, Ann Arbor, MI 48109-2125
(bpence, hfathy, stein)@umich.edu

Abstract*—This paper presents a novel method for identifying in real-time the sprung mass of a 2-DOF quarter-car suspension model. It does so by uniquely combining the base-excitation concept with polynomial chaos estimation. This unique combination of the two methods provides two important benefits. First, the base-excitation concept makes it possible to estimate the sprung mass without explicitly measuring or knowing the terrain profile prior to estimation. Second, the polynomial chaos estimation strategy makes it possible to perform such mass estimation using sprung and unsprung acceleration measurements without pseudo-integration filters that can be difficult to tune. This paper derives the proposed method in detail and presents computer simulations to evaluate its convergence speed and accuracy. The simulation results consistently converge to within 10% of the true mass value typically within 120 seconds.

I. INTRODUCTION

THIS paper examines the problem of estimating the sprung mass of an off-road vehicle online in real time. Such estimation can be valuable to online vehicle control systems such as powertrain controllers and active safety controllers. These controllers often need accurate mass estimates to optimize gear shifting, brake actuation, etc. This can be particularly critical for vehicles whose mass varies significantly between trips due to changes in cargo.

The main goal of this paper is to develop an online sprung mass estimator for vehicles that experience large changes in loading, with particular attention to off-road civilian and military trucks. Off-road driving often imparts significant vertical vibrations on such vehicles: a fact that motivates this paper's focus on using vertical vibrations to estimate vehicle sprung mass. A number of other vertical vibration-based sprung mass estimation algorithms already exist in the literature [1-8]. A detailed survey of these algorithms and their advantages and limitations appears in a previous publication by the authors [1], and is omitted here for brevity. The main contribution of this paper compared to these existing algorithms is the development of a novel method that combines the base excitation and polynomial chaos concepts [1,9] for off-road vehicle sprung mass estimation. Both the base excitation and polynomial chaos concepts have been used in previous off-road vehicle mass estimation research [1,2], but this paper uniquely combines these concepts into a single novel estimation algorithm. The remainder of this introduction briefly describes the base excitation and polynomial chaos estimation concepts, then summarizes the unique advantages of the proposed algorithm.

The concept of base excitation is borrowed from the vibrations community (see [10]) and can be interpreted within the sprung mass estimation context as the explicit treatment of unsprung motions as a vehicle vibration excitation source. Previous work by the authors used the base excitation concept in combination with recursive least squares for sprung mass estimation [1]. The resulting estimator only required sprung and unsprung acceleration measurements plus a priori knowledge of the suspension spring constant. It integrated the acceleration signals with respect to time to determine the suspension velocity and displacement. Then it filtered each of the signals with a high pass filter in order to remove the effect of integration drift. Its main limitation was the algorithm's sensitivity to the selection of the high pass filter parameters.

The polynomial chaos parameter estimation algorithm adopted in this paper was recently developed by Southward [9]. The strategy cleverly propagates the uncertainty due to unknown vehicle parameters through the suspension's dynamic equations via polynomial chaos expansions and the Galerkin method. Then it uses the "MIT rule" (a steepest descent method) to converge to parameter estimates that minimize the squared difference between the model-predicted output and the measured system output. Shimp [2], leveraging the work of Southward, used the polynomial chaos estimation (PCE) method for sprung mass estimation and experimentally validated the method, proving its feasibility for real-time applications. Shimp's work relied on prior knowledge of the ground input, which was produced by a

shaker table. Unfortunately in most applications, sufficient prior information about the ground input is not available.

This paper combines the base excitation concept with the polynomial chaos estimation (PCE) algorithm developed by Southward. This unique combination provides two important benefits. First, the base excitation concept makes it possible to estimate the sprung mass without measuring the terrain profile or knowing it a priori. Second, the polynomial chaos method makes it possible to perform such estimation using sprung and unsprung acceleration measurements only, and eliminates the need for measuring suspension velocities and displacements or estimating them using pseudo-integrators. This can be particularly attractive given the costs of suspension stroke and velocity sensors and the tuning involved in pseudo-integration.

The remainder of the paper is organized as follows: Section 2 presents the proposed mass estimation algorithm; Section 3 presents the simulations used for testing this algorithm; Section 4 presents the results of these simulations; and Section 5 provides conclusions and recommendations.

II. Solution Formulation

This section derives the proposed mass estimator by combining the base excitation concept [1,10] with the polynomial chaos estimation method proposed by Southward [9]. Part A introduces the base excitation formulation. Part B then expands the resulting base excitation model onto polynomial chaos bases. Part C applies the Galerkin projection to this expansion, and Part D concludes by developing the proposed mass estimator using the MIT rule.

A. Quarter-car Base-excitation Model

Previous work by the authors [1] proposed using the following base-excitation suspension model for sprung mass estimation. Consider a free body diagram (see Figure 1) of the sprung mass from a standard quarter car suspension system model. Furthermore, suppose that the spring stiffness coefficient k_s is a known constant and that the sprung mass m_s and suspension damping coefficient b_s are unknown. Finally, suppose that the sprung mass acceleration $\ddot{z}_s$ and unsprung mass acceleration $\ddot{z}_u$ are measured, but the suspension velocity $(\dot{z}_s - \dot{z}_u)$ and displacement $(z_s - z_u)$ are not.

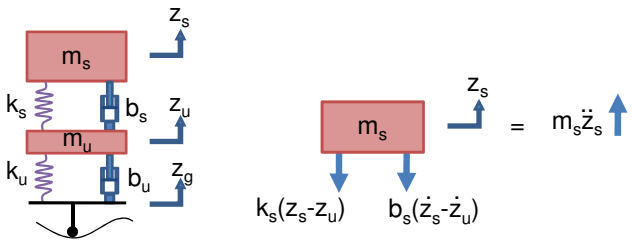

Fig. 1. Free body diagram of the sprung mass in a suspension system.

From a force analysis of the free body diagram in Figure 1, we obtain the equation:

$$m_s(\ddot{z}_s - \ddot{z}_u + \ddot{z}_u) + b_s(\dot{z}_s - \dot{z}_u) + k_s(z_s - z_u) = 0.$$

Defining $x := (z_s - z_u)$, and moving the last $\ddot{z}_u$ term to the right-hand side, the equation becomes as follows:

$$m_s\ddot{x} + b_s\dot{x} + k_s x = -m_s\ddot{z}_u. \qquad (1)$$

The measured unsprung mass acceleration $\ddot{z}_u$ is treated as the (exogenous) input to the system. The output is the measured sprung mass acceleration $\ddot{z}_s$. Define $\mu := {}^1/_{m_s}$, $x_1 := x$, and $x_2 := \dot{x}$. Then the *base-excitation* model in state-space form is the following:

$$\begin{bmatrix}\dot{x}_1\\ \dot{x}_2\end{bmatrix} = \begin{bmatrix}0 & 1\\ -k_s\mu & -b_s\mu\end{bmatrix}\begin{bmatrix}x_1\\ x_2\end{bmatrix} + \begin{bmatrix}0\\ -1\end{bmatrix}\ddot{z}_u$$
$$\ddot{z}_s = \begin{bmatrix}-k_s\mu & -b_s\mu\end{bmatrix}\begin{bmatrix}x_1\\ x_2\end{bmatrix} + [0]\ddot{z}_u. \qquad (2)$$

In this model formulation, there are two uncertain parameters which we desire to estimate simultaneously: $\mu = {}^1/_{m_s}$ and b_s. Parts B-D will present a strategy for such estimation.

B. Polynomial Chaos Expansions

Both the parameters μ and b_s of the base-excitation model and their precise statistical distributions are, in practice, unknown. However, to implement the polynomial chaos estimation procedure outlined by Southward [9], this paper assumes that both of these parameters are uniformly distributed between known upper and lower bounds, *i.e.*, $\mu_l \le \mu \le \mu_u$ and $b_{s,l} \le b_s \le b_{s,u}$.

A set of basis functions is required in order to develop a polynomial chaos expansion of the unknown parameters and state equations of Equation (2). Since by assumption the unknown parameters are drawn from the uniform distribution, Xiu and Karniadakis [11] showed that a convenient choice of polynomial basis functions is the set of Legendre polynomials over the interval [-1,1]. The first five Legendre polynomials $\phi_i(\xi), i = 0, 1, \ldots, 4$ of variable ξ are given here for convenience [12]:

$$\phi_0(\xi) = 1$$
$$\phi_1(\xi) = \xi$$
$$\phi_2(\xi) = \frac{3}{2}\xi^2 - \frac{1}{2}$$
$$\phi_3(\xi) = \frac{5}{2}\xi^3 - \frac{3}{2}\xi$$
$$\phi_4(\xi) = \frac{35}{8}\xi^4 - \frac{15}{4}\xi^2 + \frac{3}{8}$$

The Legendre polynomial $\phi_{n+1}(\xi)$ of order $n+1$ can be generated from lower-order polynomials $\phi_n(\xi)$ and $\phi_{n-1}(\xi)$ as follows[12]:

$$\phi_{n+1}(\xi) = \frac{(2n+1)\xi\phi_n(\xi) - n\phi_{n-1}(\xi)}{n+1}, \qquad n = 1,2,\ldots$$

The Legendre polynomials are orthogonal with respect to the L^2 inner product on the interval $[-1,1]$, *i.e.*,

$$\langle\phi_j(\xi), \phi_k(\xi)\rangle = \int_{-1}^{1} \phi_j(\xi)\phi_k(\xi)d\xi = \frac{2}{2j-1}\delta_{jk}$$
$$\delta_{jk} = \begin{cases}1 \text{ if } j = k\\ 0 \text{ if } j \ne k\end{cases}$$

In polynomial chaos theory, the variable ξ of the polynomials

$\phi_i(\xi), i = 0, 1, \ldots$ is viewed as being random. In this paper, the variable ξ is assumed to be drawn from the uniform distribution on the interval $[-1,1]$. The probability density function (pdf) of the random variable ξ is therefore $f(\xi) = \frac{1}{2} I_{[-1,1]}(\xi)$, *i.e.*,

$$f(\xi) = \begin{cases} 1/2 & -1 \le \xi \le 1 \\ 0 & otherwise \end{cases}$$

Viewing ξ as a uniform random variable, the inner product defined above can be interpreted as the expectation of $2\phi_j(\xi)\phi_k(\xi)$ since

$$\langle \phi_j(\xi), \phi_k(\xi) \rangle = \int_{-1}^{1} 2\phi_j(\xi)\phi_k(\xi)\frac{1}{2} d\xi = \int_{-1}^{1} 2\phi_j(\xi)\phi_k(\xi) f(\xi) d\xi = E\left[2\phi_j(\xi)\phi_k(\xi)\right].$$

Since the polynomials $\phi_i(\xi), i = 0, 1, \ldots$ are functions of the random variable ξ, they are called *polynomial chaos* functions. The goal of this section (Section 2.B) is to first expand the unknown parameters μ and b_s in terms of the polynomial chaos functions, and second, expand the base excitation equations of Equation (2) in terms of the polynomial chaos functions (see [13]).

Assume that the vehicle damping parameter is independent of its mass. Then the unknown parameters μ and b_s can be written in terms of independent variables ξ_1 and ξ_2. The variables ξ_1 and ξ_2 are uniformly distributed on the interval $[-1,1]$. Then

$$\mu(\xi_1) = \mu_0 + \mu_1\xi_1 = \mu_0\phi_0(\xi_1) + \mu_1\phi_1(\xi_1)$$

is the polynomial chaos expansion of the unknown parameter μ, and

$$b_s(\xi_2) = b_0 + b_1\xi_2 = b_0\phi_0(\xi_2) + b_1\phi_1(\xi_2)$$

is the polynomial chaos expansion of the unknown parameter b_s. The mean μ_0 and maximum variation μ_1 of $\mu(\xi_1)$ are $\mu_0 = (\mu_u + \mu_l)/2$ and $\mu_1 = (\mu_u - \mu_l)/2$ respectively. Similarly, $b_0 = (b_{s,u} + b_{s,l})/2$ is the mean and $b_1 = (b_{s,u} - b_{s,l})/2$ the maximum variation of $b_s(\xi_2)$.

Because the system parameters are uncertain, the system states and their respective derivatives are also uncertain. They can be expanded in terms of the polynomial chaos basis functions. The approximated p^{th} state and its derivative have the respective expansions:

$$\hat{x}_p(t,\xi_1,\xi_2) \approx \sum_{i=0}^{S}\sum_{j=0}^{S-i} \hat{x}_{p,\kappa}(t)\phi_i(\xi_1)\phi_j(\xi_2) \coloneqq \sum_{\kappa=0}^{\sigma} \hat{x}_{p,\kappa}(t)\Phi_\kappa(\xi_1,\xi_2)$$

and

$$\dot{\hat{x}}_p(t,\xi_1,\xi_2) \approx \sum_{i=0}^{S}\sum_{j=0}^{S-i} \dot{\hat{x}}_{p,\kappa}(t)\phi_i(\xi_1)\phi_j(\xi_2) \coloneqq \sum_{\kappa=0}^{\sigma} \dot{\hat{x}}_{p,\kappa}(t)\Phi_\kappa(\xi_1,\xi_2)$$

where S is the highest order of the polynomials $\phi_i(\xi_1)$ and $\phi_j(\xi_2)$, $\sigma = S\frac{S+3}{2}$, and $\kappa \coloneqq i\left(S + \frac{3-i}{2}\right) + j$. These are approximations of the state x_p and its derivative $\dot{x}_p$ because the expansions are truncated at a finite value σ.

The functions $\phi_i(\xi_1)$ and $\phi_j(\xi_2)$ are Legendre polynomials. Their product forms the κ^{th} basis function, i.e. $\Phi_\kappa(\xi_1,\xi_2) = \phi_i(\xi_1)\,\phi_j(\xi_2)$. The weighting functions $\hat{x}_{p,\kappa}(t)$ and their derivatives $\dot{\hat{x}}_{p,\kappa}(t)$ are functions of time but not functions of the uncertain parameters ξ_1 and ξ_2. The basis functions $\Phi_\kappa(\xi_1,\xi_2)$ are not functions of time.

The polynomial chaos expansion of the system given by Equation (2) then becomes

$$\begin{bmatrix} \dot{\hat{x}}_1(t,\xi_1,\xi_2) \\ \dot{\hat{x}}_2(t,\xi_1,\xi_2) \end{bmatrix} = \begin{bmatrix} 0 & 1 \\ -k_s\mu(\xi_1) & -b_s(\xi_2)\mu(\xi_1) \end{bmatrix} \begin{bmatrix} \hat{x}_1(t,\xi_1,\xi_2) \\ \hat{x}_2(t,\xi_1,\xi_2) \end{bmatrix} + \begin{bmatrix} 0 \\ -1 \end{bmatrix} \ddot{z}_u(t)$$

$$\ddot{\hat{z}}_s(t,\xi_1,\xi_2) = \begin{bmatrix} -k_s\mu(\xi_1) & -b_s(\xi_2)\mu(\xi_1) \end{bmatrix} \begin{bmatrix} \hat{x}_1(t,\xi_1,\xi_2) \\ \hat{x}_2(t,\xi_1,\xi_2) \end{bmatrix} + [0]\ddot{z}_u(t). \quad (3)$$

The basis functions $\Phi_\kappa(\xi_1,\xi_2), \kappa = 0,1,\ldots,\sigma$ are orthogonal [13] with respect to the inner product

$$\langle \Phi_j(\xi_1,\xi_2), \Phi_k(\xi_1,\xi_2) \rangle = \int_{-1}^{1}\int_{-1}^{1} \Phi_j(\xi_1,\xi_2)\Phi_k(\xi_1,\xi_2) d\xi_1 d\xi_2.$$

The Galerkin method exploits this orthogonality in order to numerically solve for the weighting functions $\hat{x}_{p,\kappa}(t)$ independent of the unknown parameters ξ_1 and ξ_2. This is discussed in the next section.

C. The Galerkin Method

The Galerkin projection is the process of taking the expanded equations (Equation (3)) and projecting them onto the polynomial bases. The Galerkin method separates the stochastic and time-dependent elements of the system's dynamics, thereby allowing one to solve explicitly for the time variables.

Using the inner product defined above, the state equations from Equation (3) are projected onto the polynomial basis functions. To demonstrate this, consider the projection of each component of the second state equation $\dot{\hat{x}}_2(t,\xi_1,\xi_2) = -k_s\mu(\xi_1)\hat{x}_1(t,\xi_1,\xi_2) - b_s(\xi_2)\mu(\xi_1)\hat{x}_2(t,\xi_1,\xi_2) - \ddot{z}_u(t)$ onto the polynomial basis functions.

First, the projection of $\dot{\hat{x}}_2(t,\xi_1,\xi_2)$ onto the n^{th} basis function is given by

$$\langle \Phi_n(\xi_1,\xi_2), \dot{\hat{x}}_2(t,\xi_1,\xi_2) \rangle = \langle \Phi_n, \sum_{\kappa=0}^{\sigma} \dot{\hat{x}}_{2,\kappa}(t)\Phi_\kappa \rangle$$

$$= \sum_{\kappa=0}^{\sigma} \dot{\hat{x}}_{2,\kappa}(t)\,\langle \Phi_{\mathrm{n}}, \Phi_{\kappa}\rangle$$
$$= \hat{x}_{p,n}(t)\langle \Phi_{\mathrm{n}}, \Phi_{\mathrm{n}}\rangle.$$

The last equality follows from the orthogonality of the basis functions.

The projection of $-k_s\mu(\xi_1)\hat{x}_1(t,\xi_1,\xi_2)$ onto $\Phi_{\mathrm{n}}(\xi_1,\xi_2)$ is

$$\langle \Phi_{\mathrm{n}}(\xi_1,\xi_2), -k_s\mu(\xi_1)\hat{x}_1(t,\xi_1,\xi_2)\rangle$$
$$= -k_s\left(\hat{x}_{1,n}(t)\mu_0\langle \Phi_{\mathrm{n}}, \Phi_{\mathrm{n}}\rangle + \sum_{\kappa=0}^{\sigma} \hat{x}_{1,\kappa}(t)\mu_1\langle \Phi_{\mathrm{n}}, \xi_1\Phi_{\kappa}\rangle\right).$$

The projection of $-b_s(\xi_2)\mu(\xi_1)\hat{x}_2(t,\xi_1,\xi_2)$ onto $\Phi_{\mathrm{n}}(\xi_1,\xi_2)$ is

$$\langle \Phi_{\mathrm{n}}(\xi_1,\xi_2), -b_s(\xi_2)\mu(\xi_1)\hat{x}_2(t,\xi_1,\xi_2)\rangle$$
$$= -\left(\hat{x}_{2,n}(t)\mu_0 b_0\langle \Phi_{\mathrm{n}}, \Phi_{\mathrm{n}}\rangle + \sum_{\kappa=0}^{\sigma} \hat{x}_{2,\kappa}(t)\mu_1 b_0\langle \Phi_{\mathrm{n}}, \xi_1\Phi_{\kappa}\rangle + \sum_{\kappa=0}^{\sigma} \hat{x}_{2,\kappa}(t)\mu_0 b_1\langle \Phi_{\mathrm{n}}, \xi_2\Phi_{\kappa}\rangle + \sum_{\kappa=0}^{\sigma} \hat{x}_{2,\kappa}(t)\mu_1 b_1\langle \Phi_{\mathrm{n}}, \xi_1\xi_2\Phi_{\kappa}\rangle\right).$$

And, finally, the projection of $-\ddot{z}_u(t)$ onto $\Phi_{\mathrm{n}}(\xi_1,\xi_2)$ is given by

$$\langle \Phi_{\mathrm{n}}(\xi_1,\xi_2), -\ddot{z}_u(t)\rangle = -\ddot{z}_u(t)\langle \Phi_{\mathrm{n}}(\xi_1,\xi_2), \Phi_0(\xi_1,\xi_2)\rangle = \begin{cases} -\ddot{z}_u(t)\langle \Phi_0, \Phi_0\rangle & n = 0 \\ 0 & otherwise \end{cases}$$

Thus the projection of Equation (3) onto the basis functions $\Phi_{\mathrm{n}}(\xi_1,\xi_2)$, $n = 0,1,\ldots\sigma$ results in the following equations:

$$\begin{bmatrix} \Xi & \mathbf{0} \\ \mathbf{0} & \Xi \end{bmatrix}\dot{\mathrm{X}}(t) = A_{PCE}\mathrm{X}(t) + B_{PCE}\ddot{z}_u(t) \qquad (4)$$

i.e.,

$$\dot{\mathrm{X}}(t) = A_{DET}\mathrm{X}(t) + B_{DET}\ddot{z}_u(t) \qquad (5)$$

where

$$A_{PCE} = \underset{\in\,\mathbb{R}^{2(\sigma+1)\times 2(\sigma+1)}}{\begin{bmatrix} \mathbf{0} & \Xi \\ -k_s(\mu_0\Xi + \mu_1\Xi_1) & -\mu_0 b_0\Xi - \mu_1 b_0\Xi_1 - \mu_0 b_1\Xi_2 - \mu_1 b_1\Xi_{12} \end{bmatrix}}$$

and $A_{PCE}\mathrm{X}(t)$ is the result of projecting product of the state transition matrix and the states of Equation (3) onto the polynomial basis functions.

$$B_{PCE} = \begin{bmatrix} \mathbf{0_{\sigma+1}} \\ -\langle \Phi_0, \Phi_0\rangle \\ \mathbf{0_{\sigma}} \end{bmatrix} \in \mathbb{R}^{2(\sigma+1)}$$

is the results of projecting the input matrix onto the basis functions. Note that $\mathbf{0_{\sigma}} = [0 \quad \ldots \quad 0]^{\mathbf{T}} \in \mathbb{R}^{\sigma}$.

$$\mathrm{X}(t) \triangleq \begin{bmatrix} \hat{x}_{1,0}(t) \\ \vdots \\ \hat{x}_{1,\sigma}(t) \\ \hat{x}_{2,0}(t) \\ \vdots \\ \hat{x}_{2,\sigma}(t) \end{bmatrix} \in \mathbb{R}^{2(\sigma+1)}$$

is a vector of weighting functions that are the deterministic system's states.

$$A_{DET} = \begin{bmatrix} \Xi & \mathbf{0} \\ \mathbf{0} & \Xi \end{bmatrix}^{-1} A_{PCE}$$

is the new state transition matrix for the states $\mathrm{X}(t)$.

$$B_{DET} = \begin{bmatrix} \Xi & \mathbf{0} \\ \mathbf{0} & \Xi \end{bmatrix}^{-1} B_{PCE}$$

is the new input vector. And

$$\Xi \triangleq \begin{bmatrix} \langle \Phi_0, \Phi_0\rangle & \cdots & 0 \\ \vdots & \ddots & \vdots \\ 0 & \cdots & \langle \Phi_\sigma, \Phi_\sigma\rangle \end{bmatrix} \in \mathbb{R}^{\sigma+1\times\sigma+1}$$

$$\Xi_1 \triangleq \begin{bmatrix} \langle \Phi_0, \xi_1\Phi_0\rangle & \langle \Phi_0, \xi_1\Phi_1\rangle & \ldots & \langle \Phi_0, \xi_1\Phi_\sigma\rangle \\ \langle \Phi_1, \xi_1\Phi_0\rangle & \langle \Phi_1, \xi_1\Phi_1\rangle & \ldots & \langle \Phi_1, \xi_1\Phi_\sigma\rangle \\ \vdots & \vdots & \ddots & \vdots \\ \langle \Phi_\sigma, \xi_1\Phi_0\rangle & \langle \Phi_\sigma, \xi_1\Phi_0\rangle & \ldots & \langle \Phi_\sigma, \xi_1\Phi_\sigma\rangle \end{bmatrix} \in \mathbb{R}^{\sigma+1\times\sigma+1}$$

$$\Xi_2 \triangleq \begin{bmatrix} \langle \Phi_0, \xi_2\Phi_0\rangle & \langle \Phi_0, \xi_2\Phi_1\rangle & \ldots & \langle \Phi_0, \xi_2\Phi_\sigma\rangle \\ \langle \Phi_1, \xi_2\Phi_0\rangle & \langle \Phi_1, \xi_2\Phi_1\rangle & \ldots & \langle \Phi_1, \xi_2\Phi_\sigma\rangle \\ \vdots & \vdots & \ddots & \vdots \\ \langle \Phi_\sigma, \xi_2\Phi_0\rangle & \langle \Phi_\sigma, \xi_2\Phi_0\rangle & \ldots & \langle \Phi_\sigma, \xi_2\Phi_\sigma\rangle \end{bmatrix} \in \mathbb{R}^{\sigma+1\times\sigma+1}$$

and

$$\Xi_{12} \triangleq \underset{\in\,\mathbb{R}^{\sigma+1\times\sigma+1}}{\begin{bmatrix} \langle \Phi_0, \xi_1\xi_2\Phi_0\rangle & \langle \Phi_0, \xi_1\xi_2\Phi_1\rangle & \ldots & \langle \Phi_0, \xi_1\xi_2\Phi_\sigma\rangle \\ \langle \Phi_1, \xi_1\xi_2\Phi_0\rangle & \langle \Phi_1, \xi_1\xi_2\Phi_1\rangle & \ldots & \langle \Phi_1, \xi_1\xi_2\Phi_\sigma\rangle \\ \vdots & \vdots & \ddots & \vdots \\ \langle \Phi_\sigma, \xi_1\xi_2\Phi_0\rangle & \langle \Phi_\sigma, \xi_1\xi_2\Phi_0\rangle & \ldots & \langle \Phi_\sigma, \xi_1\xi_2\Phi_\sigma\rangle \end{bmatrix}}$$

are component matrices of A_{PCE}, A_{DET}, and B_{DET}.

The following are properties of the system given by Equations (4) and (5):

a) It is deterministic because A_{DET} and B_{DET} are constant, known, deterministic matrices.
b) $\mathrm{X}(t)$ is a time-dependent vector consisting of the polynomial chaos expansion weighting functions.
c) $\begin{bmatrix} \Xi & \mathbf{0} \\ \mathbf{0} & \Xi \end{bmatrix}$ is a diagonal, invertible matrix. Each diagonal term is nonzero by definition of orthogonality, *i.e.* $\langle \Phi_i, \Phi_i\rangle \neq 0$ for all i.

Given these properties, one can solve for $\mathrm{X}(t)$ independent of the uncertain parameters via numerical integration.

With knowledge of $\mathrm{X}(t)$, the stochastic state approximations are:

$$\begin{bmatrix} \hat{x}_1(t,\xi_1,\xi_2) \\ \hat{x}_2(t,\xi_1,\xi_2) \end{bmatrix} = \mathcal{P}(\xi_1,\xi_2)\mathrm{X}(t)$$

where

$$\mathcal{P}(\xi_1,\xi_2) = \begin{bmatrix} \mathcal{p}(\xi_1,\xi_2) & 0 \\ 0 & \mathcal{p}(\xi_1,\xi_2) \end{bmatrix}$$

and

$$\mathcal{P}(\xi_1,\xi_2) = [\Phi_0(\xi_1,\xi_2) \quad \Phi_1(\xi_1,\xi_2) \quad \dots \quad \Phi_\sigma(\xi_1,\xi_2)]$$

and the approximated output equation is

$$\ddot{\hat{z}}_s(t,\xi_1,\xi_2) = \mathrm{C}(\xi_1,\xi_2)\mathcal{P}(\xi_1,\xi_2)\mathrm{X}(t)$$

with $\mathrm{C}(\xi_1,\xi_2) = [-k_s\mu(\xi_1) \quad -b_s(\xi_2)\mu(\xi_1)]$.

The output $\ddot{\hat{z}}_s(t,\xi_1,\xi_2)$ is stochastic. Its time-varying distribution is a function of the (static) distributions of the uncertain parameters ξ_1 and ξ_2.

Part D determines estimates of the uncertain parameters ξ_1 and ξ_2 using the MIT rule.

D. Estimation via the MIT Rule

Following the procedure outlined in [9], this section uses the MIT rule (a gradient-based, steepest descent method) to estimate ξ_1 and ξ_2.

First, the cost is defined as a function of the error between the measured and approximated sprung mass acceleration [9,2].

$$J = \frac{1}{2}e^2 = \frac{1}{2}\left(\ddot{z}_s(t) - \ddot{\hat{z}}_s(t,\hat{\xi}_1,\hat{\xi}_2)\right)^2$$

The MIT rule proposes updating the estimates by searching in a direction opposite the gradient:

$$\dot{\hat{\xi}}_1 = -\gamma_1 \frac{\partial J(t,\hat{\xi}_1,\hat{\xi}_2)}{\partial \hat{\xi}_1}$$

and

$$\dot{\hat{\xi}}_2 = -\gamma_2 \frac{\partial J(t,\hat{\xi}_1,\hat{\xi}_2)}{\partial \hat{\xi}_2}$$

where γ_1 and γ_2 are fixed, non-negative scalars. Then

$$\dot{\hat{\xi}}_i = \gamma_i e\left(\frac{\partial \mathrm{C}(\hat{\xi}_1,\hat{\xi}_2)}{\partial \hat{\xi}_i}\mathcal{P}(\hat{\xi}_1,\hat{\xi}_2) + \mathrm{C}(\hat{\xi}_1,\hat{\xi}_2)\frac{\partial \mathcal{P}(\hat{\xi}_1,\hat{\xi}_2)}{\partial \hat{\xi}_i}\right)\mathrm{X}(t).$$

where

$$\left(\frac{\partial \mathrm{C}(\hat{\xi}_1,\hat{\xi}_2)}{\partial \hat{\xi}_1}\right) = [-k_s\mu_1 \quad -b_s(\hat{\xi}_2)\mu_1]$$

and

$$\frac{\partial \mathrm{C}(\hat{\xi}_1,\hat{\xi}_2)}{\partial \hat{\xi}_2} = [0 \quad -b_{s,1}\mu(\hat{\xi}_1)].$$

Also,

$$\frac{\partial \mathcal{P}(\hat{\xi}_1,\hat{\xi}_2)}{\partial \hat{\xi}_i} = \begin{bmatrix} \dfrac{\partial \mathcal{P}(\hat{\xi}_1,\hat{\xi}_2)}{\partial \hat{\xi}_i} & 0 \\ 0 & \dfrac{\partial \mathcal{P}(\hat{\xi}_1,\hat{\xi}_2)}{\partial \hat{\xi}_i} \end{bmatrix}$$

where

$$\mathcal{P}(\hat{\xi}_1,\hat{\xi}_2) = [\Phi_0(\hat{\xi}_1,\hat{\xi}_2) \quad \Phi_1(\hat{\xi}_1,\hat{\xi}_2) \quad \dots \quad \Phi_\sigma(\hat{\xi}_1,\hat{\xi}_2)]$$
$$= [\phi_0(\hat{\xi}_1)\phi_0(\hat{\xi}_2) \quad \phi_0(\hat{\xi}_1)\phi_1(\hat{\xi}_2) \quad \dots \quad \phi_S(\hat{\xi}_1)\phi_0(\hat{\xi}_2)]$$

so,

$$\frac{\partial \mathcal{P}(\hat{\xi}_1,\hat{\xi}_2)}{\partial \hat{\xi}_1} = \left[\frac{\partial \phi_0(\hat{\xi}_1)}{\partial \hat{\xi}_1}\phi_0(\hat{\xi}_2) \quad \frac{\partial \phi_0(\hat{\xi}_1)}{\partial \hat{\xi}_1}\phi_1(\hat{\xi}_2) \quad \dots \quad \frac{\partial \phi_S(\hat{\xi}_1)}{\partial \hat{\xi}_1}\phi_0(\hat{\xi}_2)\right]$$

$$= \left[0 \quad \phi_1(\hat{\xi}_2) \quad \dots \quad \frac{\partial \phi_S(\hat{\xi}_1)}{\partial \hat{\xi}_1}\phi_0(\hat{\xi}_2)\right]$$

and

$$\frac{\partial \mathcal{P}(\hat{\xi}_1,\hat{\xi}_2)}{\partial \hat{\xi}_2} = \left[\phi_0(\hat{\xi}_1)\frac{\partial \phi_0(\hat{\xi}_2)}{\partial \hat{\xi}_2} \quad \phi_0(\hat{\xi}_1)\frac{\partial \phi_1(\hat{\xi}_2)}{\partial \hat{\xi}_2} \quad \dots \quad \phi_S(\hat{\xi}_1)\frac{\partial \phi_0(\hat{\xi}_2)}{\partial \hat{\xi}_2}\right]$$
$$= [0 \quad \phi_0(\hat{\xi}_1) \quad \dots \quad 0]$$

The block diagram of Fig. 2 illustrates the flow of information in the estimation procedure.

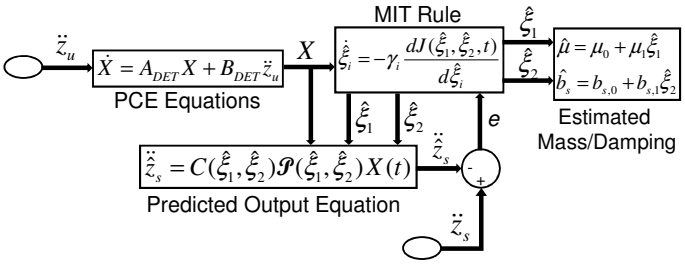

Fig. 2. The polynomial chaos estimation method.

III. Simulation-Based Demonstration

This section presents a numerical simulation framework, as shown in Figure 3, intended for demonstrating the effectiveness of estimating the sprung mass by the proposed approach. The section presents the parameters of the vehicle simulation model (in subsection 3A), the terrain model used as a source of excitation (in subsection 3B), and the structure of the estimation algorithm (subsection 3C). Section 4 then presents and discusses the simulation results.

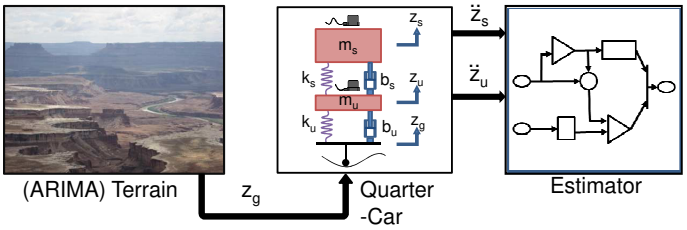

Fig. 3. The simulation setup.

A. Simulation Parameters

This paper presents simulations of the quarter-car system using parameter data from an analysis of a HMMWV vehicle (see [14]). The values used in the simulation are shown in Table 1. The suspension damping force with respect to velocity was piece-wise linear. Other system components were assumed to be linear.

TABLE I
QUARTER-CAR SIMULATION AND MODEL PARAMETERS

Symbol	Description	Value
Ts	Sampling Period	0.005 s
m_s	Vehicle sprung mass	803 kg
k_s	Suspension spring stiffness	63,528 N/m
$b_{s,ext}$	Damping coefficient for extension	3,428 N-s/m
$b_{s,cmp}$	Damping coefficient for compression	10,571 N-s/m
$\zeta_{s,ext}$	Damping ratio for extension	0.24
$\zeta_{s,cmp}$	Damping ratio for compression	0.74
m_u	Vehicle unsprung mass	98 kg
k_u	Tire stiffness coefficient	204,394 N/m
b_u	Tire damping coefficient	0 N-s/m

All units are SI: "s" indicates second; "kg" indicates kilogram; "N" indicates Newton; and "m" indicates meter.

B. The Terrain Model

This work uses an autoregressive integrated moving average ARIMA(8,1,0) model to represent an off-road terrain profile and to provide a vertical ground input z_g to the quarter-car simulation. Kern suggested this type of terrain model and gave ARIMA(8,1,0) coefficients [15]. A sample 100 meter section of the resulting terrain profile is shown in Figure 4.

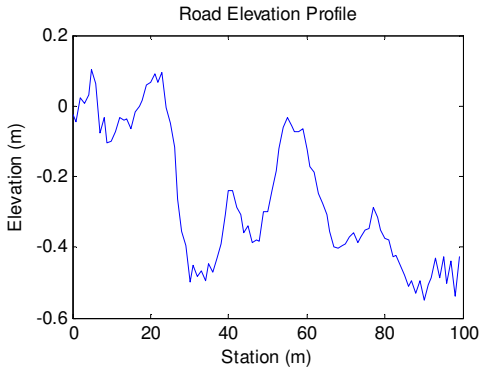

Fig. 4. 100- meter section of the terrain profile used in the simulations.

C. Estimator

A block diagram of the estimator is shown in Fig. 2. The following are design variables: γ_1, γ_2, μ_0, μ_1, $b_{s,0}$, and $b_{s,1}$. The order of the PCE equations, determined by S, is also a design variable. Unless otherwise stated, in the simulations, $\mu_0 = \frac{1}{1008}$, $\mu_1 = \frac{11}{25200}$, $b_{s,0} = 7000$, $b_{s,1} = 4500$, and $\sigma = 35$ (*i.e.* $S = 7$).

IV. SIMULATION RESULTS AND DISCUSSION

Using the simulation models from Section 3, the effect of the estimator design variables, signal noise levels, and vehicle speed on the convergence properties of the proposed estimation algorithm are presented.

The value of S (the highest order of the polynomials used in the polynomial chaos expansions, see Section 2.B) is one of the most critical variables in the PCE method. The value of S determines the value σ at which the polynomial chaos expansion is truncated. Higher values of S correspond to more accurate approximations, but the number of states (weighting functions) in the vector $\mathrm{X}(t)$ is related to S by $\dim(\mathrm{X}(t)) = 2(\sigma + 1) = 2\left(S\frac{S+3}{2} + 1\right)$. Increasing the number of states increases the computational demand. Thus S introduces a tradeoff between computational demand and estimation accuracy.

Fig. 5 and 6 illustrate the sensitivity of the PCE method to the value of S. In these figures, the error is mainly due to the truncation of the polynomial chaos expansions at a finite value. The simulation was void of signal noise and suspension nonlinearities. Instead of assuming different values for $b_{s,ext}$ and $b_{s,cmp}$ (as listed in Table I), Fig. 5 and Fig. 6 assumed that $b_{s,ext} = b_{s,cmp} = 7000\ {}^{Ns}/_{m}$. Fig. 5 shows the sensitivity of the estimate of the sprung mass to the value of S, and Fig. 6 shows the sensitivity of the estimate of the suspension damping coefficient to the value of S.

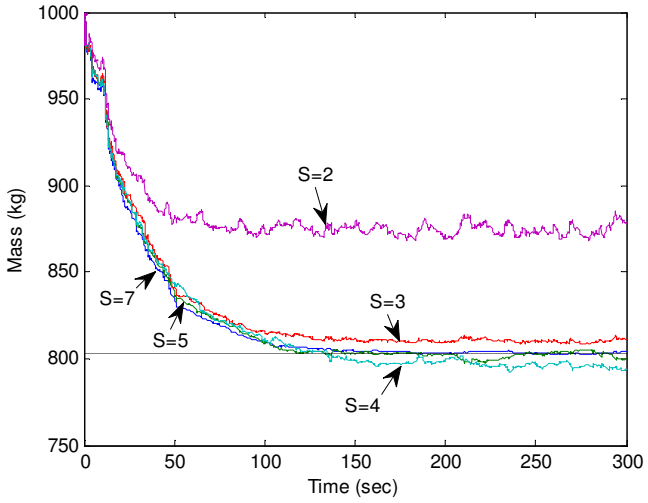

Fig. 5. Variation of sprung mass estimates with polynomial order *S*.

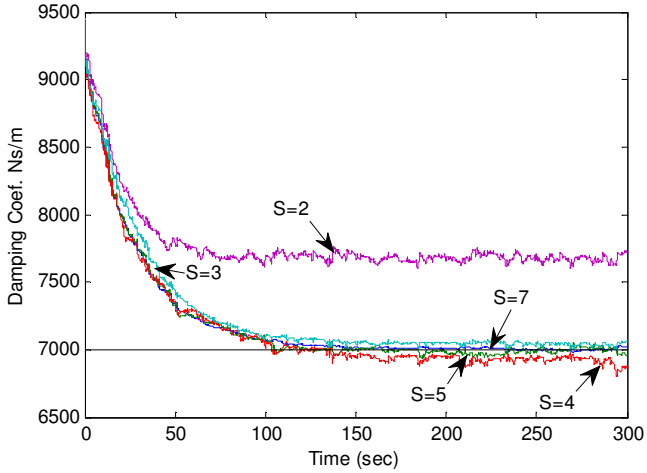

Fig. 6 Variation of damping estimates with polynomial order *S*.

As seen from Figures 5-6, as long as $S \geq 3$, the estimation errors remained less than 1.5% for mass and 3% for damping. Although not shown here, even when noise and suspension nonlinearities were added to the simulation, the estimate based on $S = 3$ was comparable to the estimate based on $S = 7$. The central processing unit (CPU) times to run the simulations in Matlab/Simulink® for $S = 2$, 3, 4, 5, and 7 were respectively 0.044, 0.055, 0.068, 0.084, and 0.123 in units of seconds of CPU time per second of simulated time. That is, it took 44 seconds of CPU time to simulate 1000 seconds when $S = 2$, etc.

For the remainder of the paper, $S = 7$, $b_{s,ext}$ and $b_{s,cmp}$ are as listed in Table I, and the simulated acceleration signals are corrupted by additive Gaussian white noise. Unless otherwise specified, both the sprung mass and unsprung mass acceleration signals were corrupted by white noise with standard deviation $\sigma_{noise} = 0.54$ m/s^2. The standard deviation of the true (*i.e.* noiseless) sprung mass acceleration signal was $\sigma_{\ddot{z}_s} = 3.6$ m/s^2, and for the unsprung mass acceleration signal $\sigma_{\ddot{z}_u} = 9.3$ m/s^2. Therefore, the signal-to-noise ratio (SNR) for the (noisy) sprung mass acceleration signal was 16dB, and for the unsprung mass acceleration, the SNR was 25dB. The SNR was calculated according to the following formula:

$$SNR = 20log_{10}\frac{stdev(signal)}{stdev(noise)}.$$

Fig. 7 illustrates the sensitivity of the PCE method to the MIT rule gains γ_1 and γ_2. In each simulation run, $\gamma_1 = \gamma_2 = \gamma$.

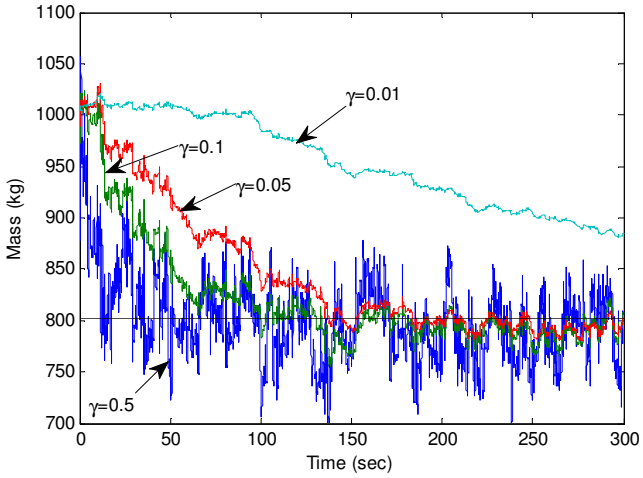

Fig. 7. Convergence of the mass estimate for varying values of the MIT rule gains γ.

As seen in Fig. 7, higher MIT rule gains improved the convergence rate, but reduced the convergence precision. Conversely, lower gains increased the precision of the estimate, but slowed the rate of convergence.

The convergence of an estimation method generally depends on the degree to which the dynamics of the system at hand are excited (see [16]). The ground input z_g is the source of excitation in the quarter-car model. Given a fixed terrain profile such as the one shown in Fig. 4, one can vary the characteristics of the ground input z_g by varying the forward velocity of the vehicle. Since the estimation measurements are acceleration signals, varying the velocity of the vehicle changes both the frequency and amplitude of the acceleration signals.

Fig. 8 shows the convergence of the estimate of mass for different values of vehicle velocity. In all cases $\gamma_1 = \gamma_2 = 0.1$. The noise standard deviation was $\sigma_{noise} = 0.73$ m/s^2 for both acceleration signals.

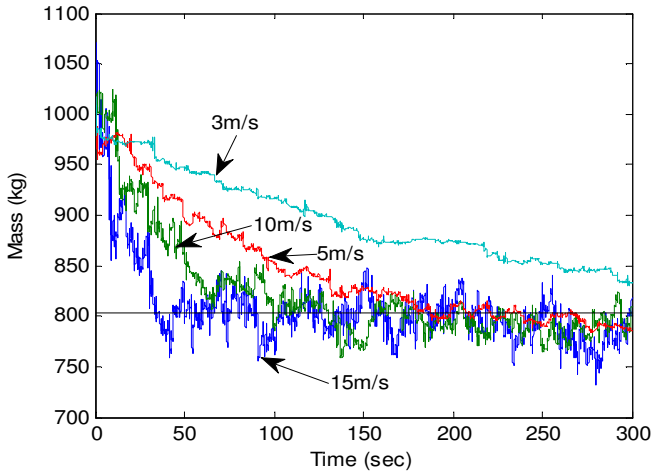

Fig. 8. Convergence of the mass estimate for varying forward velocities.

The trend in Fig. 8 shows that as the vehicle velocity increases, the convergence rate also increases. Larger amplitudes

in the ground input cause the suspension damping nonlinearity to have an observable effect on the mass estimate. Therefore, the precision of the mass estimate degrades at higher speeds.

Fig. 9 shows the effect on the mass estimate due to varying the noise standard deviation σ_{noise}. In all cases, $\sigma_{\ddot{z}_s} = 3.6$ m/s^2 and $\sigma_{\ddot{z}_u} = 9.3$ m/s^2. Higher levels of noise affected the transient part of the convergence more than on the steady state result.

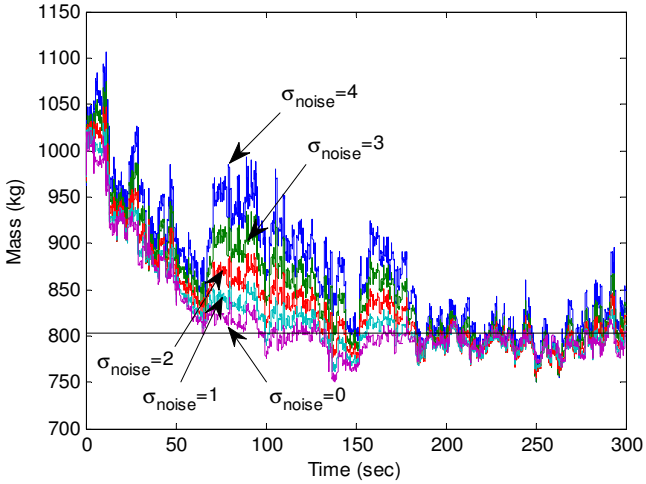

Fig. 9. The effect of noise on the estimate of sprung mass.

Finally, Fig. 10 compares a typical estimate based on the PCE method proposed in this paper with a typical estimate based on the recursive least squares (RLS) method as done in an earlier paper [1]. The RLS method converges at a faster rate, but the PCE method produces a less biased estimate.

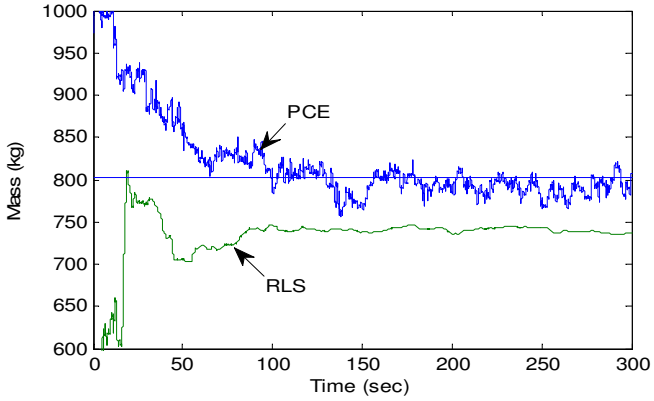

Fig. 10 the convergence of the PCE method compared with the recursive least squares method.

V. CONCLUSIONS

This paper uniquely combined base-excitation concepts with a polynomial chaos-based estimation method. Doing so provided a potential solution to real-time, off-road vehicle sprung mass estimation for situations in which the ground profile and suspension damping are not known prior to estimation. The method eliminates the need for pseudo-integration of the sprung and unsprung mass acceleration measurements, thereby also eliminating the need for pseudo-integrator tuning.

Simulation studies of a 2 degree of freedom suspension model were used to demonstrate the method. Convergence was around 120 seconds with the steady state estimate within 10% of the true sprung mass. A small tradeoff existed between convergence accuracy and computational load. This tradeoff was due to the order of the polynomial basis functions. A more significant tradeoff existed between the convergence rate and convergence precision. This tradeoff was due to the selection of the MIT rule gains. The effect of vehicle speed and signal noise was also evaluated. Overall, the simulation results suggest that the proposed base-excitation approach to polynomial chaos based estimation provides a potentially viable solution to real-time, off-road vehicle sprung mass estimation.

ACKNOWLEDGMENTS

This research was funded by the U.S. Army TARDEC through its center for excellence in automotive modeling and simulation. The authors would like to acknowledge this financial support.

REFERENCES

[1] B. L. Pence, H. K. Fathy, J. L. Stein, "Off-road Vehicle Sprung Mass Identification from Suspension Measurements", 2009 American Controls Conference, St. Louis, MO, USA

[2] S. Shimp III. "Vehicle Sprung Mass Parameter Estimation Using an Adaptive Polynomial-Chaos Method", 2008, Master's Thesis, Virginia Tech.

[3] Y. Lin and W. Kortüm "Identification of system physical parameters for vehicle systems with nonlinear components" 1992, *Vehicle System Dynamics*, 20:6, 354 — 365

[4] M. C. Best and T. J. Gordon, "Suspension System Identification Based on Impulse-Momentum Equations" 1998, *Vehicle System Dynamics* Supplement 28, pp 598-618

[5] R. Tal and S. Elad, "Method for determining weight of a vehicle in motion", 1999, U.S. Patent No. 5,973,273

[6] R. Rajamani and J. K. Hedrick, "Adaptive Observers for Active Automotive Suspensions: Theory and Experiment", 1995, IEEE Tansactions on Control Systems Technology, Vol. 3. No. 1, March 1995

[7] S. Ohsaku and H. Nakai, "Sprung Mass Estimating Apparatus" 2000, U.S. Patent No. 6,055,471

[8] K. Huh, S. Lim, J. Jung, D. Hong, S. Han, K. Han, H. Y. Jo, J. M. Jin "Vehicle Mass Estimator for Adaptive Roll Stability Control", 2007, SAE paper 2007-01-0820.

[9] S.C. Southward, "Real-Time Parameter ID using Polynomial Chaos Expansions", 2007, IMECE2007-43745

[10] D. J. Inman, *Engineering Vibration* 2nd edition, 2001, Prentice Hall, pp 113-120.

[11] D. Xiu, G. E. Karniadakis, "The Wiener-Askey polynomial chaos for stochastic differential equations", 2002, *SIAM Journal on Scientific Computing*, v 24, n 2, p 619-44.

[12] A. D. Poularikas, "The Handbook of Formulas and Tables for Signal Processing", Boca Raton: CRC Press LLC, 1999

[13] A. Sandu, C. Sandu, M, Ahmadian, "Modeling multibody systems with uncertainties. Part I: Theoretical and computational aspects", 2006, Multibody Sys. Dyn. 15:373-395

[14] Z. Lou, C. B . Winkler, R. D. Ervin, F. E. Filisko, P. J. Th. Venhovens, G. E. Johnson, "Electrorheology for Smart Automotive Suspensions" June 1994, UMTRI-94-15 pg.23-24

[15] J. V. Kern, "The Development of Measurement and Characterization Techniques of Road Profiles", 2007, Master's Thesis, Virginia Polytechnic Institute and State University

[16] P. A. Ioannou, J. Sun, *Robust Adaptive Control*, 1996 Prentice Hall, Inc. pp 250-310.